Brief Communications

A mechanistic perspective of atmospheric oxygen sensitivity on composite energetic material reactions

Cory W. Farley [a], Michelle L. Pantoya [a,*], Valery I. Levitas [b]

[a] Department of Mechanical Engineering, Texas Tech University, Lubbock, TX 79424, USA
[b] Iowa State University, Departments of Aerospace Engineering, Mechanical Engineering and Material Science and Engineering, Ames, IA 50011, USA

ARTICLE INFO

ABSTRACT

Solid energetic composites have been used and studied in standard air environments, yet the contribution of atmospheric oxygen to reactive material combustion has not been investigated. This study experimentally examines the effect of atmospheric oxygen concentration (4% or 93% oxygen) on energy propagation of nanometric aluminum with copper oxide (Al + CuO), iron oxide (Al + Fe$_2$O$_3$), calcium iodate (Al + Ca(IO$_3$)$_2$), and iodine pentoxide (I$_2$O$_5$). In all cases energy propagation was examined in terms of flame speed and higher in the high oxygen environments. However, the convectively dominant reactions showed a smaller percent increase in flame speed mainly attributed to the reaction mechanism.

© 2013 The Combustion Institute. Published by Elsevier Inc. All rights reserved.

1. Introduction

The influence of oxygen in the atmosphere has been studied for aluminum (Al) combustion either as an aerosolized powder or single Al particles [1–3]. However, there are minimal studies examining the effect of environment on flame speeds of composite fuel and oxidizer powders. Yet, in practice, energetic composites are often used in atmospheric conditions such that the role of oxygen in the environment influencing the combustion should be well understood.

When Al fuel particles are on the nanometric scale and combined with a solid oxidizer, such as a metal oxide, fluoropolymer, or halogen oxide, the flame propagation rate can exceed 100 m/s and sometimes exceed 1000 m/s [4]. For these high heating and flame rates (i.e., speeds >10 m/s), the melt dispersion mechanism (MDM) has been reported to operate [4–7]. Thus, melting of Al is accompanied by a 6% volume increase and produces pressure of several GPa in Al melt and tensile stresses of 10 GPa in the oxide shell, which cause fast fracture and spallation of the shell. Immediately after spallation, pressure inside the liquid Al particle remains the same, while at the bare Al surface it drops almost to zero. This creates an unloading wave with a tensile pressure of 3–8 GPa, which disperses Al particles into a large number of small, bare Al fragments. Oxidation of these fragments is not limited by diffusion

through initial oxide shell, which explains extremely high reaction rate. For micron scale Al reactions with a very slow heating rate and flame rates (i.e., <10 m/s) the classical diffusion oxidation mechanism operates [3,8]: reaction rate is limited by diffusion of oxygen and Al toward each other through the growing oxide shell.

This study examines the influence of atmospheric oxygen as a function of reaction mechanism. Experiments are limited to four energetic composites; two representing reaction via the MDM and two via classic diffusion oxidation. The first two composites produce high flame speeds, activate the melt dispersion mechanism, and are composed of aluminum with either copper oxide or iodine pentoxide (Al + CuO and Al + I$_2$O$_5$, respectively). It should be noted here that to achieve flame speeds comparable to Al + I$_2$O$_5$, the CuO selected for these experiments was on the nanoscale particle size. This enabled us to examine multiple powders with flame speeds greater than 100 m/s that we could classify as "fast burning powders". The second set results in significantly lower flame speeds such that the diffusion oxidation mechanism governs reaction propagation. These composites are aluminum combined with iron oxide or calcium iodate (Al + Fe$_2$O$_3$ and Al + Ca(IO$_3$)$_2$, respectively). These reactions initiate when oxygen is released from the oxide and available to react with the aluminum, however CuO and I$_2$O$_5$ dissociate at temperatures near or below the melting temperature of Al while Fe$_2$O$_3$ and Ca(IO$_3$)$_2$ dissociate at higher temperatures [9]. The objective is accomplished through high speed imaging of flame rates in controlled oxygen concentration environments. These experiments are coupled with analytical modeling of

* Corresponding author. Fax: +1 8067423540.
  E-mail address: michelle.pantoya@ttu.edu (M.L. Pantoya).

the alumina passivation shell fracture temperature such that ignition temperatures for the reaction can be correlated to the reaction mechanism.

2. Methods

2.1. Experimental

Passivated aluminum (Al) with a nominal average diameter of 80 nm and an active Al content of approximately 75 wt% was supplied by Novacentrix (formerly Nanotechnologies), Austin, TX. The oxide thickness was calculated to an average 4.0 nm and TEM images of these particles are consistent with this estimation. The Al particles were used for all tests reported here and mixed with either 50 nm average diameter CuO, 40 μm Fe_2O_3, 15 μm $Ca(IO_3)_2$ or I_2O_5 that is ground and sieved through a 355 μm mesh. All powders were supplied by Sigma Aldrich, St. Louis MO or Alfa Aesar, Ward Hill, MA. All reactions were balanced based on oxygen transfer assuming 100% of the oxygen transferred to the Al.

Individual reactant powders were prepared for stoichiometric equivalence ratios. Reactant powders were loaded into a 0.5 by 13 cm notch with a bulk density of 7% of the theoretical maximum density (TMD) of the solid mixture meaning 93% of the volume in the notch is occupied by atmospheric gas. For each test, three to five experiments were performed to establish repeatability, which was found to be the largest source of uncertainty in the data.

The experimental setup includes a sealed combustion chamber with a blow-off valve to prevent pressurization as seen in Fig. 1. Two roughing pumps were connected to the sealed combustion chamber and one third of the atmosphere was vacuumed out and backfilled with either argon (Ar) or oxygen (O_2). This atmospheric cycle was repeated 4 times for the argon and 6 times for the oxygen resulting in a High O_2 content of 93% O_2 by mass and a low O_2 content of 4% by mass. Therefore, when the sample is ignited, the atmosphere is either 4 or 93% O_2 and at atmospheric pressure. Ignition was triggered via a heated nickel chromium hot wire. Flame speeds were recorded via a Phantom 7 high speed camera at frame rates ranging from 900 to 90,000 frames per second aligned perpendicular to the direction of flame propagation. The pixels were converted to millimeters via calibration and combined with the frame rate to calculate flame speed.

2.2. Theoretical

To further understand the influence of reaction mechanism on sensitivity to atmospheric oxygen, the temperature for which oxide shell fractures and melt disperses for Al in a reaction involving MDM can be determined theoretically. The key geometric parameter that governs the MDM is the ratio of Al core, R, to the oxide shell thickness, δ; $M = R/\delta$ For $M < 19$, entire particle melts
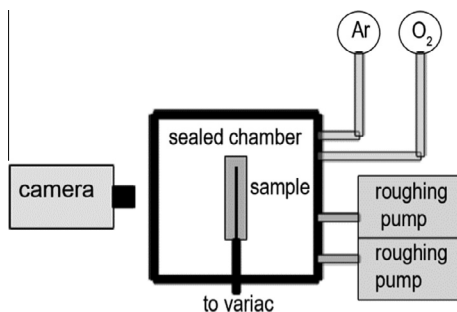
completely before oxide fracture and entire melt disperses and participate in reaction. The maximum tensile hoop stress in the shell (considered as the negative one) is determined by Eq. (1) [5,10]:

$$\sigma_h = -\frac{6(m^3+2)(\varepsilon_2^i - \varepsilon_1^i)G_2K_1K_2}{H} + \frac{4(m^3+2)G_2K_2\Gamma_1}{RH} + \frac{(2\Gamma_2 + p_g Rm)m^2(-2G_2K_1 + 3(2G_2 + K_1)K_2)}{RH}, \quad (1)$$

where subscripts 1 and 2 designate Al and alumina, respectively, $m = 1 + 1/M$, Γ_1 and Γ_2 are the surface energies at the core-shell and shell-gas interfaces, G and K are the shear and bulk moduli, $K_1 = fK_1^m + (1-f)K_1^s$ is the bulk modulus of Al melt (m) - solid (s) mixture, f is the concentration of melt in Al particle, and $H = 3m^3K_{1-}K_2 + 4G_2(K_1 + (m^3 - 1)K_2)$. For convenience, it is assumed that compressive stress is positive and that tensile stress is negative. Inelastic strain consists of thermal and transformational parts:

$$\varepsilon_1^i = -(\alpha_s(T_m - T_0) + (1-f)\alpha_s(T - T_m) + f\alpha_m(T - T_m) + f\varepsilon^m); \varepsilon_2^i = -\alpha_2(T - T_0), \quad (2)$$

where α is the linear thermal expansion coefficient, T_0 is the temperature at which the initial oxide shell was formed on the solid Al particle (i.e., temperature at which internal thermal stresses in the solid state are zero), and $3\varepsilon^m$ is the volumetric expansion during the melting of Al. For the MDM, the temperature at which fracture of the oxide shall occurs during continuous heating can be determined from fracture criterion

$$\sigma_h = -\frac{6(m^3+2)(\varepsilon_2^i - \varepsilon_1^i)G_2K_1K_2}{H} + \frac{4(m^3+2)G_2K_2\Gamma_1}{RH} + \frac{(2\Gamma_2 + p_g Rm)m^2(-2G_2K_1 + 3(2G_2 + K_1)K_2)}{RH} = -\sigma_u \quad (3)$$

by putting $f = 1$, where σ_u is the ultimate strength of alumina. All material parameters are presented in [5]; in particular, $\sigma_{th} = 11.33$ GPa, $T_0 = 300$ K and $p_g = 0$.

3. Results

Table 1 displays the flame speeds for the mixtures organized by equivalence ratio and atmosphere. In order to compare flame speeds, a percent difference is defined in Eq. (4) where FSH is the flame speed under 93% O_2 conditions and FSL is the flame speed for 4% O_2 conditions.

$$\% \text{ Increase} = \frac{FSH - FSL}{FSL} * 100\% \quad (4)$$

For 80 nm Al particles used here, $R = 40 - \delta$ and $M = (40 - \delta)/\delta$. Substituting these expressions in Eq. (3) foe the MDM and resolving for T the temperature at which oxide shell fractures versus shell thickness δ is shown in Fig. 2 and can be well approximated by linear relationship in Eq. (5),

$$T = 945 + (\delta - 2)(1449 - 945)/3, \quad (5)$$

which passes through points $T = 945$ K at $\delta = 2$ nm and $T = 1449$ K at $\delta = 5$ nm. In reality, there is a broad range of distribution of particle size and oxide thickness. Even if we assume for

Fig. 1. Experimental schematic for flame speed experiments.

Table 1
Summary of flame speed results from each set of tests with speeds in (m/s).

	Al + I_2O_5	Al + CuO	Al + $Ca(IO_3)_2$	Al + Fe_2O_3
93% O_2	840 ± 40	224 ± 4	2.9 ± 0.04	3.4 ± 0.1
4% O_2	770 ± 20	204 ± 9	2.2 ± 0.05	1.7 ± 0.04
% Increase	9%	10%	30%	100%